Anisotropic Rescaling of a Splayed Pinning Landscape in Hg Cuprates: Strong Vortex Pinning and Recovery of Variable Range Hopping

L. Krusin-Elbaum,[1] G. Blatter,[2] J. R. Thompson,[3] D. K. Petrov,[1] R. Wheeler,[4] J. Ullmann,[5] and C. W. Chu[6]
[1]*IBM Research, Yorktown Heights, New York 10598*
[2]*ETH-Hönggerberg, CH-8093 Zürich, Switzerland*
[3]*Oak Ridge National Laboratory, Oak Ridge, Tennessee 37831*
and Department of Physics, University of Tennessee, Knoxville, Tennessee 37996
[5]*UES Incorporated, Dayton, Ohio 45432*
[6]*Los Alamos National Laboratory, Los Alamos, New Mexico 87545*
[7]*Texas Center for Superconductivity, Houston University, Houston, Texas 77204*
(Received 10 June 1998)

Strong vortex pinning by fission-induced uniformly splayed columnar tracks in anisotropic mercury cuprates is demonstrated to result from (re)scaling of the pinning landscape by a large superconducting anisotropy. The effective "narrowing" of the splay distribution restores variable range vortex hopping (VRH) motion expected for nearly parallel pins. VRH emerges as a distinctive peak in the vortex creep rate ($\sim$12% at low fields at $T/T_c \sim 0.5$) of the most anisotropic $HgBa_2Ca_2Cu_3O_{8+\delta}$, a peak well described by a glassy dynamics with the characteristic exponent $\mu \sim 1/3$. [S0031-9007(98)07526-7]

PACS numbers: 67.40.Vs

An outcome of an extensive effort [1] to counteract easy vortex wandering in high temperature superconductors [2] is the realization that a random array of parallel crystallographic columnar defects localizes vortices best over largest regions of the H-T space [3,4]. However, for such an array, thermally activated vortex motion (creep)—via nucleation and subsequent spreading of the double-kink vortex excitations [3]—takes advantage of the vast available phase space for hopping processes. Indeed, a variable-range vortex hopping (VRH) [5] (analogous to the variable range motion in doped semiconductors [6]) to the energetically equivalent (parallel) tracks can be surprisingly fast [4,5]. To inhibit the fast VRH channel, Hwa *et al.* [7] came up with an ingenuous theoretical idea relying on strong localizing action of columnar pins, namely forcing topological vortex entanglement [8] by splaying the track directions, i.e., giving them an angular spread. This would pin vortex kink pairs, and reduce hopping by reducing the number of parallel pinning sites.

Recent tests of these ideas [9–12] demonstrate large supercurrent (J_c) enhancements and suppressed vortex dynamics by splayed columnar pins in a 3D (three-dimensional, albeit anisotropic) $YBa_2Cu_3O_{7-\delta}$ (YBCO) [9,10]. There, the pinning is optimal only for sufficiently small splay angles [9] $\theta \simeq 10°$, consistent with topologically entangled vortices [11,12]. However, the consequence of a large-θ splay in a 3D system is severe—by destroying vortex coherence along the field direction [11] it *reduces* the pinning action to that of point defects [9,11]. On the other hand, *large boosts* of supercurrents, and especially large shifts of the irreversibility line by a large-angle (or uniform) splay in quasi-2D $Bi_2Sr_2CaCu_2O_8$ (BSCCO) [10,13], and by uniformly splayed tracks in highly anisotropic $HgBa_2CaCu_2O_{6+\delta}$ (Hg-1212) [14], are not well understood in the context of entanglement [7,10,11]. This invites a basic question about the interplay between strong correlated disorder, anisotropy, and structural (polycrystalline) disorder.

Here we demonstrate that the complexity of randomly oriented columnar defects in a polycrystalline material is elegantly removed by a large superconducting anisotropy, restoring the generic physics and the relative simplicity of crystals with parallel pins. We show that strong vortex pinning by a uniform (large-θ) splay in anisotropic Hg cuprates (large J_c enhancements and a shift of the irreversibility line to T' s > 110 K) is a consequence of *anisotropic rescaling of the pinning landscape*. As a result, a rescaled—"focused"—distribution of splay angles effectively leads to the recoupling of the vortex segments [11,15] and to a recovery of variable range vortex hopping through such splay with increasing anisotropy—motion expected only for an array of nearly aligned pins [3,7].

We use a nuclear fission process [16] of Hg as a tool to install uniformly splayed pinning tracks [14] in mercury cuprates $HgBa_2Ca_{n-1}Cu_nO_{2n+2+\delta}$ with $n = 1$, 2, or 3 adjacent CuO layers (Hg-1201, –1212, or –1223) [17]. The three polycrystalline Hg cuprates, with closely alike starting morphology [18], were exposed to a 0.8 GeV proton beam from the WNR branch of LAMPF at Los Alamos National Laboratory. The corresponding superconducting anisotropy parameters [2] γ estimated at $\sim$ 20, $\sim$ 50, and $\sim$60 [19], span the range between YBCO and BSCCO. The virgin materials, prepared following Ref. [18], have sharp resistive T_c's: $\sim$95 K for Hg-1201, $\sim$120 K for Hg-1212, and $\sim$127 K for Hg-1223. The p^+ fluences in the range $1.3–3.0 \times 10^{17}$ p^+ cm^2 were determined to $\sim$2% from proton-induced ^{24}Na activation of thin Al foils facing each sample during its irradiation. The cross-sectional and

 0031-9007/98/81(18)/3948(4)$15.00

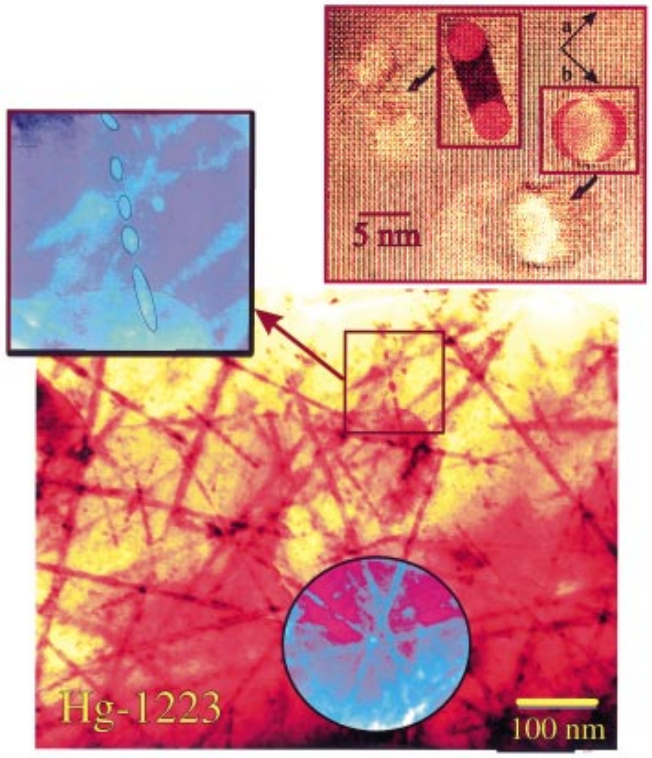

FIG. 1(color). (a) Transmission electron micrograph (TEM) of a Hg-1223 sample exposed to a p^+ fluence of $1.2 \times 10^{17}/\text{cm}^2$. Circular enclosure highlights uniform large splay. Inset (left): A bubblelike track typical of morphology near the ends of the ion ranges [1]. The track density in the TEM is $\approx 3.4 \times 10^{10}/\text{cm}^2$. With fission cross section $\sigma_{\text{Hg}} = 100$ mbarns and Hg density $\rho_{\text{Hg}} \approx 4.3 \times 10^{21}/\text{cm}^3$, the density of fission events is 5.2×10^{13} fiss./cm^3 and an estimated mean track length is ~ 6.6 μm for *two* fission fragments. Inset (right): High resolution lattice TEM image (of ~ 100 Å thick sample) illustrates the variation (5–9 nm) of amorphous track diameters.

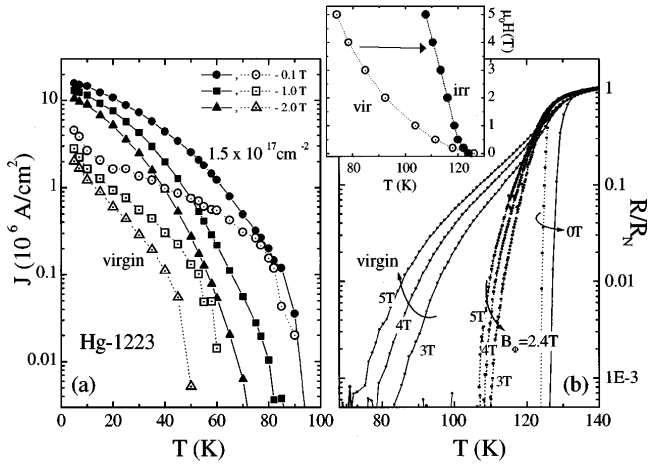

FIG. 2. (a) The persistent current density $J(T)$ for Hg-1223 sample before and after irradiation with $1.5 \times 10^{17}/\text{cm}^2$ proton fluence ($B_\Phi \sim 1.2$ T), for three values of H. J was obtained from magnetization M, as in Ref. [9], using TEM determined grain size (~ 20 μm). (b) Resistance R (normalized) before and after irradiation with $B_\Phi \sim 2.4$ T. For $H \neq 0$ (i) the onset of linear dissipation is shifted to higher temperatures, and (ii) R (at any fixed T) is much lower after the p^+ exposure. At this B_Φ, T_c is reduced by ~ 3 K. Inset: Irreversibility lines obtained from the nonlinear I-V characteristics using a 1 μV/cm criterion.

lattice transmission electron microscopy (TEM) images in Fig. 1 highlight the prominent features of the p^+-launched fission-track landscape: a random large-splay-angle distribution, and the variation in track diameters.

The effect on current conduction in the most anisotropic Hg-1223 is large. Figure 2a shows the persistent current density J vs temperature before irradiation and after. Here, the defect density corresponds to a matching field (1 vortex per 1 defect) $B_\Phi = 1.2$ T. In the virgin sample the high-field J drops fast—at $\mu_o H = 2$ T the current is essentially null for temperatures beyond ~ 50 K (as in Hg-1212 [14]). The current boost due to the p^+ exposure is over 2 orders of magnitude at 1 T and ~ 60 K. A substantial expansion of the irreversible regime is illustrated in Fig. 2b—the vanishing of linear resistivity (onset of J_c) for $B_\Phi = 2.4$ T is up-shifted by ~ 40 K to $T \gtrsim 110$ K at a 4 T field (see inset).

The effect on the thermal time relaxation of J is shown in Fig. 3, which compares the *normalized* creep rates (recorded as in Ref. [5]) $S = -d \ln J / d \ln t$ for the three Hg cuprates before irradiation and with the same $B_\Phi \sim 1.2$ T. We note two significant points. First, the creep rate is suppressed by p^+ irradiation in Hg-1223 and Hg-1212, but *not* in Hg-1201 [14]. And second, after irradiation we witness a *new dynamical feature*, namely a large peak in S at ~ 60 K $\sim 0.5 T_c$—emerging for Hg-1212 and fully developing for Hg-1223—a peak strikingly similar to the one observed in YBCO with *parallel* tracks [5]. In what follows we point out that both effects are connected to the different anisotropies of these cuprates. In the least anisotropic Hg-1201, vortex dynamics is *enhanced* by a large splay, as also observed in YBCO with large-θ splay distributions [9]. Indeed, both experiments and numerical simulations in YBCO show that large-θ defect crossings (or close encounters) can promote kink nucleation, and hence stimulate creep [9]. But the emergence of a "$\|$-pin-YBCO-like" peak in the creep rate of the most anisotropic Hg-1223 with fission tracks is enigmatic at first glance. Below we use the anisotropic scaling approach [20] to show that a key to this is in the collusion of random columnar-pin landscape and large anisotropy.

Consider an individual grain in a ceramic material subject to an external magnetic field $\mathbf{H}$. The grain contains irradiation tracks homogeneously distributed over all angles. Now we ask when such a grain will strongly pin by trapping vortices on the tracks. The result will depend on the track pinning efficiency η [4,5], the anisotropy γ, the pin density (controlled by p^+ fluence), the magnitude B of the induction, and on the angle θ_B between the field and the $\hat{\mathbf{c}}$ axis of the grain. We follow the path outlined in Ref. [2]

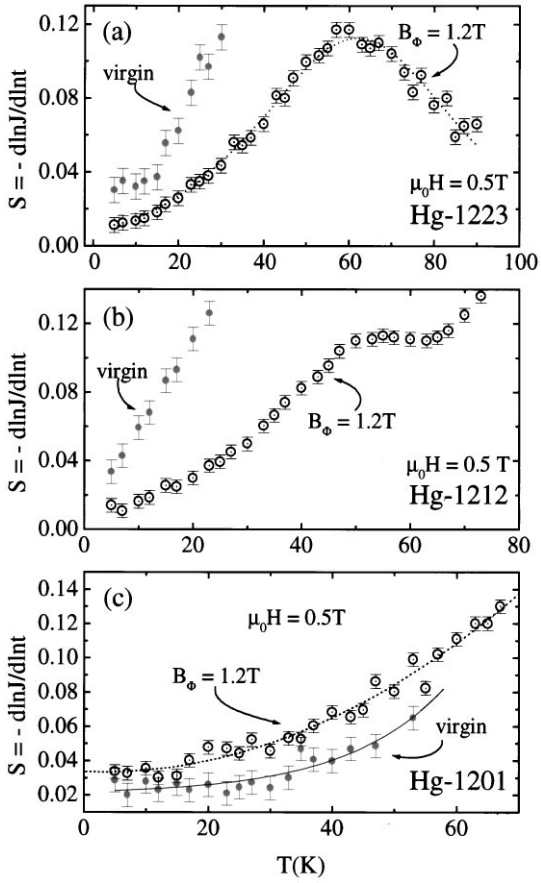

FIG. 3. Relaxation rates $S(T)$ at $H = 0.5$ T for (a) Hg-1223, (b) Hg-1212, and (c) Hg-1201 before irradiation and after, *all* with $B_\Phi \sim 1.2$ T. Only the *intra*grain pinning is relevant. A 12% peak is well articulated for the most anisotropic Hg-1223. In the irradiated Hg-1201 creep is *enhanced*.

and map the grain with its tracks and magnetic field to an isotropic system. We proceed in three steps: (i) rescale the field, (ii) rescale the distribution of splay angles $\mathcal{P}(\theta)$, (iii) derive a strong pinning condition for the ceramic.

(i) The first step immediately gives [20] (in the grain coordinate system) $\tilde{B} = \gamma_{\theta_B} B/\gamma$, where $\gamma_{\theta_B}^2 = \sin^2\theta_B + \gamma^2 \cos^2\theta_B$. In the isotropized system, the vortices are aligned along $\tilde{\theta}_B = \arctan(\gamma^{-1}\tan\theta_B)$; after rescaling, in most grains the field is pointing in the direction of the $\hat{\mathbf{c}}$ axis with an angular spread $\sim 1/\gamma$.

(ii) The rescaled splay-angle distribution follows from $\tilde{\mathcal{P}}(\tilde{\theta})\sin\tilde{\theta}d\tilde{\theta} = \mathcal{P}(\theta)\sin\theta d\theta$ (the planar angle φ is not modified under the scaling transformation) and $\tan\tilde{\theta} = \gamma^{-1}\tan\theta$. The original distribution is isotropic in angle, i.e., $\mathcal{P}(\theta) = 1/2$. Upon rescaling, the angular distribution of tracks is strongly forward peaked,

$$\tilde{\mathcal{P}}(\tilde{\theta}) = \frac{\gamma^2/2}{(\cos^2\tilde{\theta} + \gamma^2\sin^2\tilde{\theta})^{3/2}}, \qquad (1)$$

defining a *focused-track cone* (FTC) of width $\sim 1/\gamma$ directed along the $\hat{\mathbf{c}}$ axis (e.g., half of the tracks end up in the angular regime $\tilde{\theta} < \sqrt{3}/\gamma$). In general, within an angle $\tilde{\theta}_0$ we find the fraction

$$p(\tilde{\theta}_0) = 2\int_0^{\tilde{\theta}_0} d\tilde{\theta}\sin\tilde{\theta}\tilde{\mathcal{P}}(\tilde{\theta}) = 1 - \frac{\cos\tilde{\theta}_0}{\sqrt{\gamma^2\sin^2\tilde{\theta}_0 + \cos^2\tilde{\theta}_0}} \qquad (2)$$

of all the tracks. Since the tracks have diameters larger than 2ξ (i.e., the vortex cores fit into the tracks at all angles), we will have strong pinning tracks at all angles in the isotropized system, $\tilde{\epsilon}_r \approx \eta\varepsilon_0$, where ε_0 is the line energy, $\tilde{\epsilon}_r$ is the track pinning energy, and $\eta \approx 0.2$ (an estimate for Hg-1223 can be obtained from $J_c \sim \eta J_o$ [17], where J_o is the depairing current; see also Refs. [4,5]).

(iii) The vortices are strongly pinned by tracks pointing along $\tilde{\theta}_B$ within a *trapping cone* of width $\tilde{\theta}_t \approx \alpha\sqrt{2\tilde{\epsilon}/\tilde{\varepsilon}_l}$ [2]. Here, $\alpha < 1$ is a trapping parameter set by, e.g., a restricted trapping length or vortex-vortex interactions, and the isotropized line tension $\tilde{\varepsilon}_l \approx \varepsilon_0$. For the strong pinning tracks of (ii) we then obtain a trapping cone (TC) of width $\sim\sqrt{2\eta}\alpha$ [21]. The relevant parameter is set by the *overlap* of the focused-track and the trapping cones. We first concentrate on the strong-pinning/large-anisotropy regime when the TC encloses the FTC, characterized by the condition $\sqrt{2\eta}\alpha\gamma > 1$. The fraction $p(\tilde{\theta}_t)$ of tracks available for strong pinning gives an upper estimate for the effective matching field of the ceramic

$$B_\Phi^{\rm cer} \lesssim p(\tilde{\theta}_t)B_\Phi \approx \left[1 - \frac{1}{\sqrt{1 + 2\eta\alpha^2\gamma^2}}\right]B_\Phi . \qquad (3)$$

If the effective pinning parameter $\sqrt{2\eta}\alpha\gamma$ falls below unity (e.g., due to a smaller anisotropy γ) the FTC broadens beyond the TC and only a fraction $\sim\eta\alpha^2\gamma^2$ of the tracks in the FTC participates in strong pinning, in agreement with the rapid decrease of $B_\Phi^{\rm cer}$ in (3).

An independent estimate $\alpha \sim 0.1$ for the trapping parameter is obtained from $\theta_t^2 \cong 2\eta\alpha^2\gamma^2$ by using YBCO parameters: $\gamma \sim 5$ and $\theta_t \simeq 10°$ [9]. This places the least anisotropic Hg-1201 at 0.5 T in the weak pinning regime (3) [above $B_\Phi^{\rm cer}$]. The strongly anisotropic Hg-1223 with $\gamma \gtrsim 60$ resides well within the strong pinning region, consistent with the experiment.

So now rescaling in the most anisotropic Hg-1223 brings us back to almost parallel defects. A prominent correspondence of the large (12%) creep peaks in YBCO with $\parallel$ pins where the peak is due to VRH (see [5]), and in Hg-1223 with fission-induced tracks is consistent with rescaling to forward-θ. Both occur well below T_c at $\sim 0.5T_c$ and only at fields below B_Φ. The dispersion in track energies evident from Fig. 1 will give rise to the VRH vortex motion in the glassy solid [3,6].

To search for the VRH motion we probe the glassy dynamics in Hg-1223 via the current dependence of the effective activation energy for vortex hopping, $U(J)$ [3,5]. $U(J)$ obtained using Maley's scheme [22] is plotted in Fig. 4 for $\mu_0 H = 0.5$ T. In a glassy phase [2] the

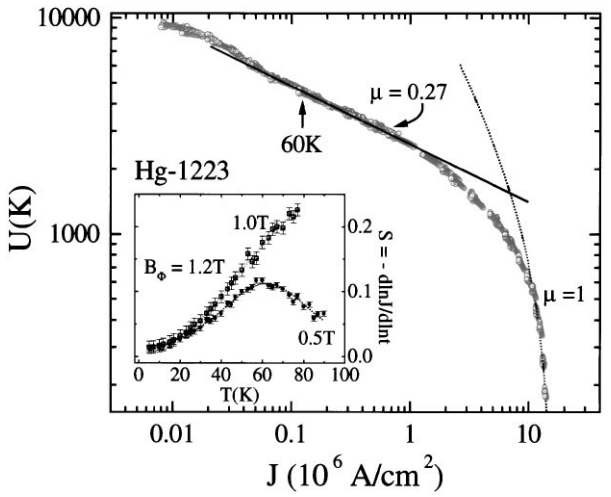

FIG. 4. Effective activation energy $U(J)$ for Hg-1223 with $B_\Phi = 1.2$ T. At $\mu_0 H = 0.5$ T—as in a single-crystal YBCO with $\|$ pins [5]—$U(J)$ shows a large regime with the slope $\mu \sim 1/3$ (solid line is a fit to $\mu = 0.27 \pm 0.02$ between 30 and 70 K), characteristic of the variable range motion (VRH) in the region of the creep peak. Dashed line is a fit to $U(J)$ near J_c [2] with $\mu \simeq 1$, indicative of half-loop regime [3]. Inset: The creep peak disappears for $\mu_0 H > B_\Phi$.

activation barriers $U(J)$ at small currents behave as $U(J,T) \propto (J_c/J)^\mu$. Figure 4 shows that as J decreases, $U(J)$ gradually crosses to an extended current regime [$J \approx (0.05 - 1) \times 10^6$ A/cm^2], where large segments of $\ln U(J)$ vs $\ln J$ are linear. The slope provides an estimate of $\mu = 0.27 \pm 0.02$, to be compared with the predicted value of $1/3$ in the VRH regime [3] in the temperature vicinity of the creep peak [5]. And, as in YBCO [5], at high fields the peak in S disappears (inset Fig. 4). An estimated *maximum* thermal creep rate at the peak $S^{\max} \sim [\mu \ln(t/t_{\rm eff})]^{-1}$, with $\mu = 0.27$ and $\ln(t/t_{\rm eff}) \simeq 26$ (see note in [23]), is $S^{\max} \sim 0.12$, in good agreement with our data. The creep rate is slower than in the virgin material, which may reflect entanglement of the recoupled vortices by a small "remnant" splay [9].

In summary, using *uniformly* splayed pinning landscape as a tool in the same family of Hg cuprates we (i) demonstrate that such correlated disorder pins vortices *stronger* in materials with *higher* anisotropy γ and (ii) formulate a consistent description of this systematic trend via a *scaling approach* [2], which allows one to estimate the strength of pinning with changing γ. This reconciles our observations with the theoretical proposals regarding splay and may help guide practical delivery schemes of efficient pinning sites into anisotropic superconductors.

We thank V. M. Vinokur for useful remarks. This work was supported in part by EPRI Contract No. RP-8065-11 and by NSF GOALI Grant No. DMR-9510731. Work at ORNL was sponsored by the U.S. DOE under Contract No. DE-AC05-96OR22464 with Lockheed Martin Energy Research Corp.

[1] See review of L. Civale, Supercon. Sci. Technol. **10**, 11 (1997), and references therein.
[2] G. Blatter *et al.*, Rev. Mod. Phys. **66**, 1125 (1994).
[3] D. R. Nelson and V. M. Vinokur, Phys. Rev. B **48**, 13 060 (1993); Phys. Rev. Lett. **68**, 2398 (1992).
[4] L. Krusin-Elbaum *et al.*, Phys. Rev. B **53**, 11 744 (1996).
[5] J. R. Thompson *et al.*, Phys. Rev. Lett. **78**, 3181 (1997).
[6] B. I. Shklovskii and A. L. Efros, *Electronic Properties of Doped Semiconductors* (Springer, New York, 1984).
[7] T. Hwa *et al.*, Phys. Rev. Lett. **71**, 3545 (1993).
[8] D. R. Nelson, Nature (London) **385**, 675 (1997).
[9] L. Krusin-Elbaum *et al.*, Phys. Rev. Lett. **76**, 2563 (1996); L. Civale *et al.*, Phys. Rev. B **50**, 4102 (1994).
[10] V. Hardy *et al.*, Physica (Amsterdam) **257C**, 16 (1996).
[11] D. López *et al.*, Phys. Rev. Lett. **79**, 4258 (1997).
[12] W. K. Kwok *et al.*, Phys. Rev. Lett. **80**, 600 (1998).
[13] L. Krusin-Elbaum *et al.*, Appl. Phys. Lett. **64**, 3331 (1994); H. Safar *et al.*, *ibid.* **67**, 130 (1995).
[14] L. Krusin-Elbaum *et al.*, Nature (London) **389**, 243 (1997), and references therein. The p^+ irradiation reduces low-field J in Hg-1201; see Physica (Amsterdam) **282C**, 375 (1997).
[15] M. Sato *et al.*, Phys. Rev. Lett. **79**, 3759 (1997).
[16] F. D. Becchetti *et al.*, Phys. Rev. C **28**, 276 (1983); T. Gabriel (private communication). Typical fission offspring of $^{200}_{80}$Hg would be $^{90}_{40}$Zr and $^{93}_{41}$Nb at ~100 MeV.
[17] A. Schilling *et al.*, Nature (London) **363**, 56 (1993); J. R. Thompson *et al.*, Phys. Rev. B **54**, 7505 (1996).
[18] Q. M. Lin *et al.*, Physica (Amsterdam) **254C**, 207 (1995); Q. Xiong *et al.*, J. Appl. Phys. **76**, 7127 (1994).
[19] D. Zech *et al.*, Phys. Rev. B **53**, R6026 (1996); G. Le Bras *et al.*, Czech. J. Phys. **46**, 1769 (1996).
[20] G. Blatter, V. Geshkenbein, and A. I. Larkin, Phys. Rev. Lett. **68**, 875 (1992).
[21] This analysis assumes track lengths l_t larger than the typical trapping length $r_t \simeq \sqrt{\Phi_0/B_\Phi}/\tilde{\theta}_t$ [2], a condition well satisfied in the present situation.
[22] M. P. Maley *et al.*, Phys. Rev. B **42**, 2639 (1990). Maley's scheme uses the master rate equation $U(J,T) = -kT[\ln(dM/dt) - C]$. Here $C = \ln(2dB/\tau_0 L) = 25$, $d = \sqrt{\Phi_0/B_\Phi} = 415$ Å, and $L \sim 20$ μm. At $\mu_0 H = 0.5$ T the microscopic attempt time $\tau_0 \sim 4 \times 10^{-11}$ sec.
[23] The characteristic *macroscopic* time [2] $t_{\rm eff} \approx (TL^2/c|\partial U/\partial J|aH)\tau_0 \sim 10\tau_0$ is obtained with $\partial U/\partial J \sim U_0/J_c$, $T/U_0 \sim 0.03$, $L/a \sim 0.3 \times 10^3$, and $H \sim J_c L/c$ (see Ref. [5]).